EurJIC European Journal of Inorganic Chemistry

DOI: 10.1002/ejic.201200525

Inorganic–Organic Hybrid Materials Based on Amino Acid Modified Hydrotalcites Used as UV-Absorber Fillers for Polybutylene Succinate

Christian Coelho,*[a] Thomas Stimpfling,[a] Fabrice Leroux,*[a] and Vincent Verney[a]

Keywords: Organic–inorganic hybrid composites / Layered compounds / Amino acids / Nanostructures / Rheological behavior

Polybutylene succinate (PBS)-functionalized nanocomposites with amino acid tyrosine (TYR)- and tryptophan (TRY)-hybrid-interleaved layered double hydroxide (LDH) materials exhibit interesting anti-UV properties and rheological properties. Embedding amino acid into the layered double hydroxide container preserves the UV shielding property of the pristine organic molecule. When employed in an aliphatic polymer such as PBS, chain scission occurs during photoageing and accelerates the degradation of the raw material. However the embedded inorganic amino acid melt blended with PBS prevents such degradative phenomenon. An investigation of their structure–property relationship (i.e., nonmiscibility and expanded PBS nanocomposite structures) was conducted. The nonmiscible structure observed for LDH-TYR was found to be associated with a chain-extender behaviour, whereas the interleaved structure of PBS-LDH-TRY yielded a liquid–gel transition. Both PBS nanocomposite structures were found to be stable under agressive UV conditions, whereas amino acid free of an LDH container resulted in a deleterious effect when dispersed in PBS, largely promoting PBS chain scission. Hence amino acid organically modified hydrotalcites appear to hold promise for use as UV absorbers when dispersed into other aliphatic biodegradable polymers.

Introduction

Biodegradable polymers have been widely investigated to replace synthetic polymers, which generate large amounts of waste and also lead to ecological problems. They are generally derived from polyesters such as polybutylene adipate terephthalate, poly(ε-caprolactone) or poly(lactic) acid. Inherently aliphatic polyesters merit considerable attention because they present the highest rate of biodegradability and have properties that mimic those of traditional thermoplastics.[1] One of the most commonly studied aliphatic polyesters is polybutylene succinate (PBS), which is obtained by the direct polycondensation of succinic acid and butane-1,4-diol in the presence of catalysts such as $Ti(OiPr)_4$, $Al(OiPr)_3$, Sn, $SnCl_2$ or distannoxanes.[2] Applications are widespread from biodegradable fibres to packaging materials and injection moulded products and bottles. Biotic degradation is expected but abiotic degradation such as photooxydation should be limited to keep the bulk properties intact as long as possible. After study by matrix-assisted laser desorption ionization time-of-flight mass spectrometry, the mechanism of photooxidation was explained from an oxidation of hydroxy end group, hydrogen-abstraction decomposition and Norrish I photocleavage.[3]

Some organic additives called light stabilizers could be used to prevent the photodegradation of the polymer. They are classified into two categories: UV absorbers, which absorb in the ultraviolet region with transferable protons such as benzophenones, benzotriazoles or benzene sulfonic acids, and hindered amine light stabilizers, which slow down the hydroperoxidation process by acting like antioxidants.[4] However, their incorporation directly into the polymer leads to several drawbacks: the possible reaction of the organic molecule directly with the polymer, thereby leading to the scission of its chain and diffusion of the additive out of the polymer. There is a topical and ever-growing interest in combining sustainable solutions to develop materials without having to compromise on the required properties. Such a challenge can be reached by the use of a "green filler". The idea is to encapsulate the organic UV absorber within an inorganic framework, thus protecting the polymer chain from the degradative action of the organic molecules and finally leading to an inorganic–organic (I/O) hybrid assembly. The use of a nanocontainer that features a large aspect ratio, in addition to suppressing degradation, might prevent migration and subsequent creation of porosity within the polymer network as well as its leaching out of the polymer. Organic–inorganic hybrids based on clay minerals such as smectites, sepiolites or layered double hydroxides have been used as building blocks for assembling organic molecules in nanostructured materials.[5,6]

[a] Institut de Chimie de Clermont Ferrrand, (ICCF)-UMR 6296, Université Blaise Pascal,
24 avenue des Landais, 63177 Aubière (Cedex), France
Fax: +33-4-73407169
E-mail: christian.coelho@univ-bpclermont.fr
fabrice.leroux@univ-bpclermont.fr
Homepage: http://iccf.univ-bpclermont.fr/

Supporting information for this article is available on the WWW under http://dx.doi.org/10.1002/ejic.201200525.

Hydrotalcite-like compounds, also known as "anionic clays" or "layered double hydroxides", can endow the UV-shielding property quite easily. They constitute a large family of materials with the general formula $[M^{II}_{1-x}M^{III}_{x}(OH)_2](A_{n-x/n})\cdot mH_2O$ in which M^{II} is a divalent cation such as Mg, Ni, Zn, Cu or Co and M^{III} is a trivalent cation such as Al, Cr or Fe, with A^{n-} being an anion of charge n such as CO_3^{2-}, Cl_-, NO_3^- or an organic anion. The structure is assembled into brucite-like sheets in which the interlayer anions can easily be exchanged. It has been reported that layered double hydroxide (LDH) nanofillers are efficient candidates to host organic chromophores that contain carboxylic or sulfonic groups.[7,8]

From the point of view of polymer chemistry, organically modified hydrotalcites can act as a reactive nanofiller and create weak or strong interactions.[9] The tendency has recently been used to combine functionalities. New functionalized polymers were designed by incorporating an I/O assembly. Poly(ε-caprolactone) composites that contain benzoate LDHs presented good antimicrobial properties.[10] LDH nanofillers were found to have a strong interfacial attrition with PBS[11] and polylactic acid.[12] Other properties such as fire retardation, gas permeability and biocompatibility can be achieved with such an approach.[13]

To the best of our knowledge, several studies deal with I/O hybrids that act as UV absorber of traditional polymers such as polypropylene or poly(vinyl alcohol)[14–16] but no studies concern biodegradable polymers. Biological molecules such as derivatives of benzoic acid, sulfonic acid and cinnamic acid intercalated in layered double hydroxides were successfully tested as UV sunscreens.[17–20] Amino acids are interesting biological candidates since they combine a transferable proton and amine function, two important criteria for UV-shielding functionality. Due to their zwitterionic forms, they can be easily incorporated into both anionic and cationic clays. They have been interleaved into several inorganic systems as Ni–Al, Mg–Al and Zn–Al layered double hydroxides,[21–24] respectively, and into montmorillonite host structures.[25,26] When above their isoelectric point, amino acids can act as anionic species that could be easily intercalated into hydrotalcite sheets. The influence of pH was previously discussed in terms of degree of crystallinity and the degree of incorporation of anionic glutamate into hydrotalcite interlayers.[27] The free deprotonated amino function could confer certain features onto the I/O assembly such as creating a molecular container for pharmaceutical agents[21] or event conductivity and catalytic properties.[22] Some amino acids other than glycine were successfully delaminated in the presence of formamide,[22] thereby indicating that amino acids might be an efficient organo-modifying agent that is able to result in exfoliation of the LDH platelets and thus reinforce some mechanical and barrier properties. Recently, strong attrition was observed by melt rheology between glycine or alanine LDHs and silicone chains,[28] which could open the door to functionalization of other materials that feature a strong interaction with amino acid inorganic hybrids. LDH host structures were recently developed as biocompatible inorganic nanoparticle carriers for cells that contain large amino acid macromolecules such as collagen peptides or myoglobin.[29,30]

For this study, well-defined and large-aspect-ratio Zn_2Al layered double hydroxide (LDH) nanofillers were chosen to host amino acids: L-tryptophan (TRY) or L-tyrosine (TYR). Characterizations were performed by X-ray diffraction and diffuse reflectance UV spectroscopy on the LDH/TRY and LDH/TYR inorganic–organic structures as well as of the PBS nanocomposite structure when dispersed as 5% into PBS through a twin-screw extruder. The associated UV-shielding properties of the functionalized PBS nanocomposite were evaluated by transmission and emission spectroscopic measurements after various exposure times. Additionally, rheological experiments assessed the macromolecular evolution upon irradiation. The study emphasizes the use of an inorganic container to render the chemical functionality more robust when the polymer is exposed to aggressive conditions.

Results and Discussion

I/O Hybrid Material Properties

The organically modified LDH that contains the levogyre form amino acids L-TRY and L-TYR were prepared by coprecipitation methods. XRD patterns of the corresponding I/O hybrid LDH assemblies are presented in Figure 1.

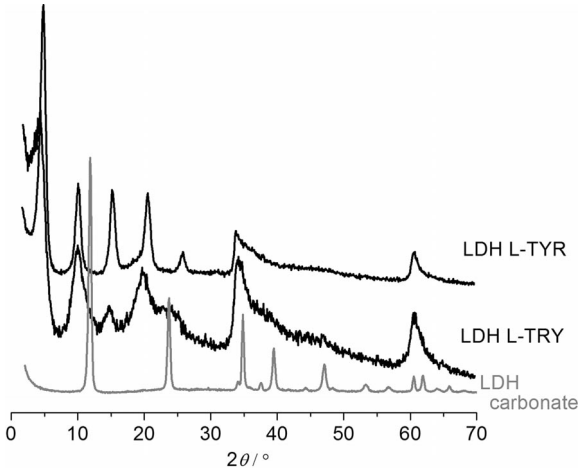

Figure 1. XRD patterns of (Zn,Al)–CO_3 LDH, (Zn,Al)-TRY LDH, (Zn,Al)-TYR LDH.

(Zn,Al)–CO_3 LDH presents a basal spacing value of 0.76 nm (2θ = 11.6°). When L-TRY and L-TYR are coprecipitated in the (Zn,Al)-LDH host structure, basal spacings increase to 1.95 (2θ = 4.5°) and 1.71 nm (2θ = 5.2°), respectively. These values are in agreement with those found in the literature.[21–23] The XRD patterns of (Zn,Al)-TRY and (Zn,Al)-TYR indicate no more diffraction peaks of the carbonate phase; they show a complete intercalation of amino acids and no carbonate contamination.

By estimating the molecular length of L-TRY and L-TYR to be approximately 1 nm and the LDH gallery thickness to be 0.47 nm,[31] a more precise geometry of the arrangement of the amino guest species inside the LDH galleries can be assessed. The organic anions are uncoiled inside the lamellar structure and positioned in a perpendicular orientation with respect to the hydroxide layers. This is in agreement with previous molecular simulations performed on (Mg,Al)-LDH that contains tyrosine.[26] Anions are separated by 0.6 nm from each other and they prefer an edge-to-face orientation, thus forming a hydrophobic region in the midplane with the presence of benzene rings. Additionally, from Figure 1, the stronger signal-to-noise response for LDH-L-TYR indicates that this hybrid phase presents a greater coherence length, which means that its associated stacking sequence is more regularly ordered than that of LDH-L-TRY.

Counterintuitively, hybrid LDH-L-TYR presents a specific Brunauer–Emmett–Teller (BET) surface area of 69.4 $m^2 g^{-1}$, which is greater than 17.9 $m^2 g^{-1}$ for LDH-L-TRY or 23.4 $m^2 g^{-1}$ for LDH carbonate. Higher BET surface-area values for L-TYR were previously found for LDH and montmorillonite hosts.[31,32]

The UV-absorbing properties of amino acids L-TYR and L-TRY when they are embedded into inorganic LDH structures are presented in Figure 2. In the absence of amino acid chromophore, the LDH host structure presents no absorption process. Subtle changes occur in the UV domain when amino acids are confined between inorganic platelets. For L-TRY, the maximum absorption shifts from 306 to 296 nm when intercalated in LDH. As for L-TYR chromophore, an opposite and more pronounced bathochromic shift from 285 to 302 nm is observed. Such a shift is typical of a specific arrangement called J-type aggregates inside the inorganic matrix.[33] The preliminary analyses indicate that LDH-L-TYR and LDH-L-TRY can act as UV absorbers and, due to the interesting form factor supplied by LDH platelets, they might act as an efficient filler in polymer technology and engineering.

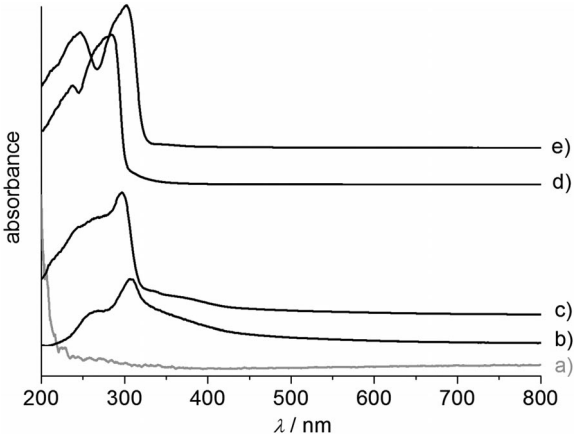

Figure 2. Diffuse reflectance UV/Vis spectra (Kubelka–Munk functions) of (a) (Zn,Al)–CO_3, (c) (Zn,Al)-TRY and (e) (Zn,Al)-TYR. For comparison, the diffuse reflectance UV/Vis spectra of (b) L-tryptophan and (d) L-tyrosine are provided.

I/O Hybrid Materials/PBS Nanocomposites

The XRD pattern of PBS blended with amino acid LDH are given in Figure 3. The diffraction peak at 19.7° (d = 4.51 Å) is ascribed to the (020) diffraction plan for PBS monoclinic crystal (Figure S1 in the Supporting Information).[34] The dispersion of the I/O hybrid does not affect the crystallinity of PBS or the coherence length.

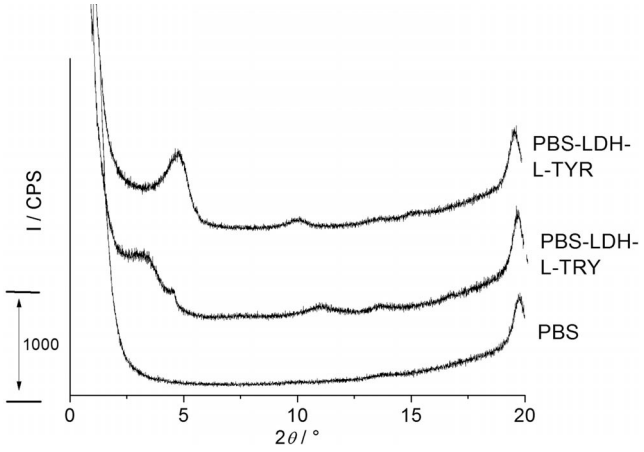

Figure 3. XRD patterns of PBS, PBS-LDH-L-TRY and PBS-LDH-L-TYR.

The basal spacings are 1.79 and 2.87 nm for PBS-LDH-L-TYR and PBS-LDH-L-TRY, respectively. The PBS polymer chain diffuses inside the lamellar inorganic platelet, thus leading to an expansion of the basal spacing for PBS-LDH-L-TRY. For PBS-LDH-L-TYR, the basal spacing was identical to the (Zn,Al)-TYR nanohybrid, which means that the mixture was not miscible in this case.

UV/Vis transmittance spectra of PBS nanocomposites are presented in Figure 4. The addition of (Zn,Al)–CO_3 did not affect the UV properties of PBS nanocomposites, which means that the inorganic structure is totally unreactive towards the polymer chain, thus showing that any shift will be caused by the organic chromophores.

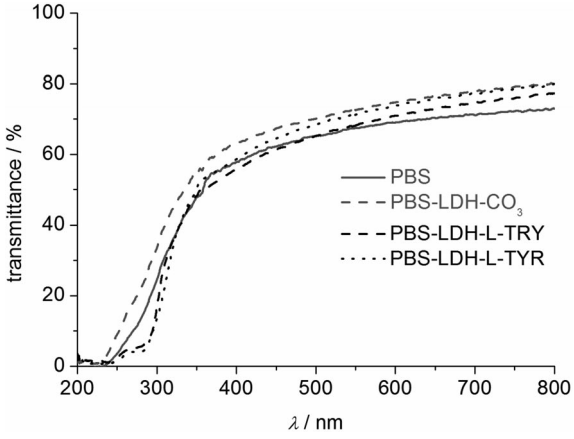

Figure 4. UV/Vis transmittance spectra of PBS nanocomposites.

The large decrease in transmittance at 300 nm for PBS-LDH-L-TRY and PBS-LDH-L-TYR comes from the strong absorption band of the amino acid chromophores, as de-

scribed previously. Both L-TRY and L-TYR seem to act as UV absorber when embedded into (Zn,Al) hydrotalcite types. The result is not presented here but evidently pristine amino acid chromophores, when directly dispersed into PBS, confer the same UV transmittance spectra onto PBS blends relative to PBS nanocomposites. This observation supports the idea that the inorganic host is optically inert towards the polymer chain.

The microstructural changes were scrutinized by rheology in the molten state (Figure 5). From the Cole–Cole formalism, the shift of the depressed semicircle towards smaller values of η' and η'' for L-TYR and L-TRY dispersed into PBS indicates the greater ease of the polymer chain for relaxation, thus indicating a plasticizing effect. This is evidently not suitable for PBS applications.

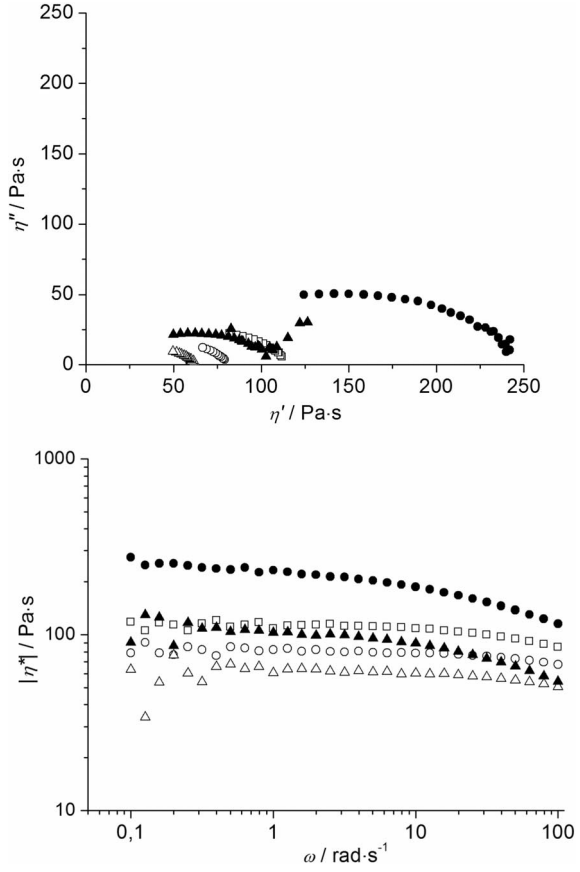

Figure 5. Viscoelastic behaviour of PBS (□), PBS-L-TYR (○), PBS-L-TRY (Δ), PBS-LDH-L-TYR (●), PBS-LDH-L-TRY (▲).

In contrast, a large increase in η'_0 and higher values of complex viscosities observed for LDH-L-TYR filler underlines the chain-extending effect associated with the nonmiscible structure. The free hydroxy function in the tyrosine molecule could participate in this phenomenon through the chain mobility of PBS-LDH-L-TYR. This has previously been hypothesized for cinnamic derivatives.[19]

By contrast, the η''–η' curve for PBS-LDH-L-TRY exhibits a semicircle portion superimposable upon PBS without filler and a straight line in the low-ω region. The latter feature is ascribed to the formation of a gel-like structure. By comparing the complex viscosity versus the shear frequency, it can be noted that a shear-shinning behaviour is expected for this intercalated structure, accompanied by a strong restriction to the relaxation of the polymer chain. PBS chains are strongly immobilized in the vicinity of the LDH-L-TRY, which suggests a greater interface developed between the tethered L-TRY and PBS.

Evolution of Polymeric Properties towards UV Ageing

To assess the durability of PBS nanocomposites towards UV ageing, the structure was evaluated by X-ray diffraction after photoageing time (i.e., 70 h; Figure S2 in the Supporting Information). There is no detectable change to the (020) reflection peak—neither in position nor in intensity—after irradiation of PBS nanocomposite films.

After irradiation, the diffraction peak attributed to the LDH hybrid filler is located in the same position, even if a subtle decrease in intensity was noticed. This means that the crystallinity of PBS nanocomposites is not affected by the ultraviolet rays. The thermograms of PBS nanocomposites before and after photoageing strengthen this statement (Figure S3 in the Supporting Information). From a structural point of view, PBS seems to be unaffected, whereas the

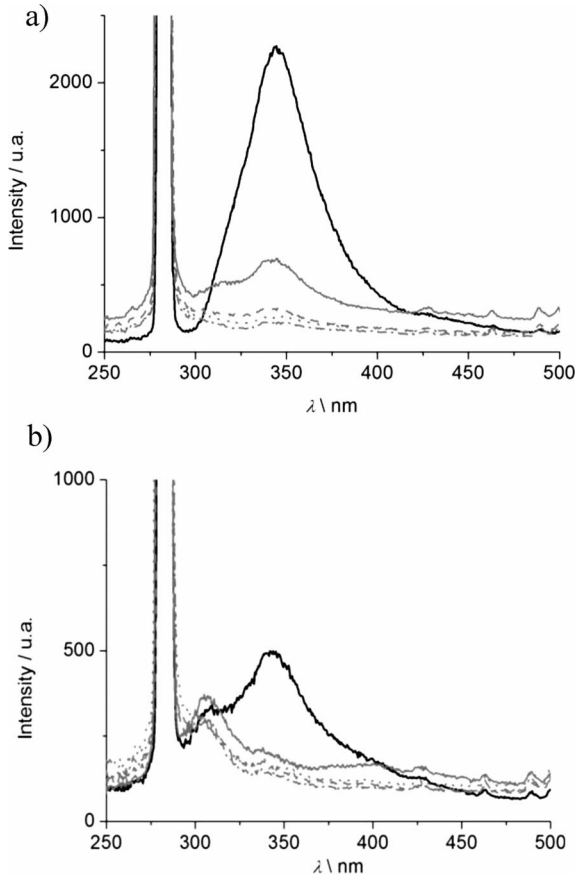

Figure 6. Fluorescence spectra of PBS nanocomposites with I/O hybrids (a) LDH-L-TRY and (b) LDH-L-TYR for various exposure times 0 (—), 10 (—), 20 (- - -), 40 (···) and 70 h (–·–). Excitation was set at 280 nm.

hybrid filler seems to undergo delamination, as previously observed in a formamide environment,[22] or platelets break down but are associated to no visible byproduct.

To disentangle such hypotheses, molecular emission spectroscopy and melt rheological measurements were conducted on the irradiated I/O hybrid material/PBS.

From Figure 6 it can be seen that an intense emission band centred at 350 nm is evidenced in the fluorescence spectra of PBS nanocomposites with LDH L-TYR or LDH-L-TRY. This fluorescence is attributed to the emission of the amino acid adsorbed on the surface of the LDH or to the interlayered molecule.[35] For PBS-LDH-L-TRY, the observed decrease in fluorescence intensity upon UV exposure is not quantitatively noticeable due to the heterogeneity of the films. Interestingly, for PBS-LDH-L-TYR, the emission band shifts towards the lower wavelength of 305 nm, which corresponds to the traditionally observed emission of L-TYR.[30] This emission is also observed when L-TYR is dispersed with PBS (Figure S4 in the Supporting Information). This observation indicates that LDH-L-TYR is present in a different microenvironment after UV irradiation, thus confirming that delamination of the platelets could have occurred.

When PBS blends with both amino acids, L-TYR and L-TRY are photoaged and complex viscosity largely decreases with a pronounced shear thinning effect in the low-ω (Figure 7), thus indicating that chain scission occurs simultaneously with the formation of a gel-like structure. The shear thinning parameters n are calculated in the low ω (Table S1 in the Supporting Information) by taking into account the hypothesis of $|\eta^*|$ tending to ω^n and reaching a plateau in the low ω if the polymer behaves like a quasi-Newtonian liquid ($n = 0$). These antagonist mechanisms also occur in pristine PBS films, as discussed elsewhere.[3,20] In the Supporting Information (Figure S5 in the Supporting Information), the shift η' versus η'' whole curve to lower values and therefore of η'_0 supports this affirmation. Moreover the cross-linking phenomenon is also observed by a straight line in the low-ω region of the Cole–Cole plot.

To the contrary, PBS blends with amino acid embedded in the inorganic brucite sheets feature on the whole the same viscous patterns upon UV exposure. PBS-LDH-L-TRY and PBS-LDH-L-TYR keep their ability to flow, with a slight shear thinning effect observed upon irradiation for the intercalated structure with LDH-L-TRY, which is intrinsic to its microstructure. Interestingly, this attrition upon irradiation is not observed with the nonmiscible structure (PBS-LDH-L-TYR).

LDH platelets are found to maintain the microstructural integrity of PBS under radiation stress by preventing the chain scission of PBS and partially keeping the macromolecular motion of the viscous part of PBS.

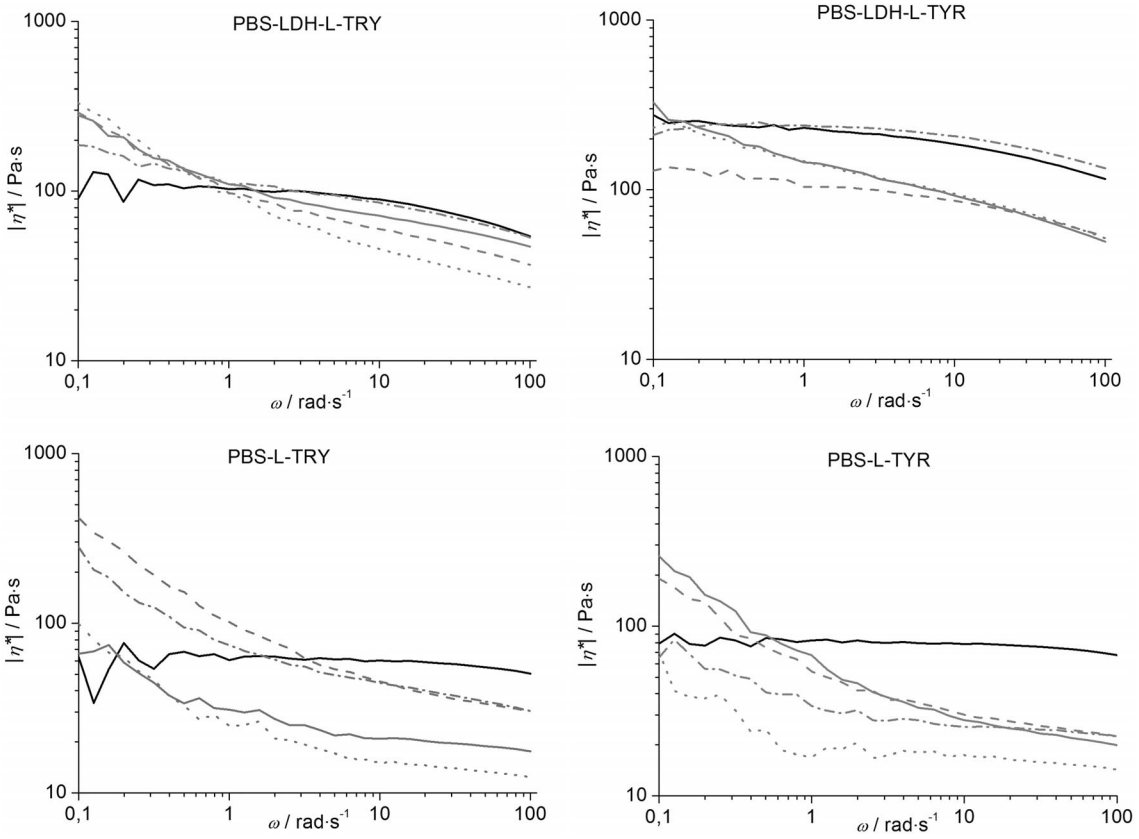

Figure 7. Complex viscosity versus ω for blends of PBS with both amino acids and their I/O hybrids for various UV exposure times: 0 (—), 10 (—), 20 (- - -), 40 (···) and 70 h (—·—).

Conclusion

By combining rheological and X-ray diffraction measurements with studies of UV-absorption properties, new functionalized PBS nanocomposites were successfully characterized. The combined use of L-tryptophan or L-tyrosine embedded in layered double hydroxides with PBS prevented chain scission from happening under photoageing tests. This means that amino acid hybrid LDHs are efficient candidates for use as UV sunscreen additives through melt blending. Both nonmiscible and expanded structures are observed that are not modified after UV-irradiation treatment. Melt rheology indicates that some macromolecules of PBS nanocomposites behave like a gel structure after being damaged by UV irradiation, but the viscous character is not affected, which is indicative of a rather strong stability towards photoageing by means of hybrid LDH filler dispersion.

Experimental Section

General: The guest molecules, L-tyrosine (hereafter called TYR, isoelectric point (pI) = 5.7) and L-tryptophan (TRY, pI = 5.9) were obtained from Aldrich and used as received.

The host substances Zn–Al LDH were prepared on the basis of coprecipitation by keeping pH constant to 6.5–7.0 (pH > pI).[23,27] $ZnCl_2$ and $AlCl_3{\cdot}6H_2O$ were mixed with milliQ water (100 mL). Solutions of NaOH and organic guest were added dropwise with vigorous stirring under a nitrogen atmosphere. The molar ratio of $Zn^{2+}/Al^{3+}/OH^-$/organic guest was 2:1:5:1. The reaction mixture was subsequently centrifuged, washed with water and oven-dried at 30 °C for 24 h. The molecular formulae of the LDH amino acids were $Zn_2Al(OH)_6$[L-tyrosine]·$2H_2O$ (M_r = 475.96 g mol^{-1}) and $Zn_2Al(OH)_6(OH)_6$[L-tryptophan]·$2H_2O$ (M_r = 499.03 g mol^{-1}).

Polybutylene succinate (PBS) was used as commercially received. PBS/LDH/amino acid were obtained at 120 °C by melt blending PBS (95% w/w) and LDH/amino acid (5% w/w) in a twin screw extruder Hakke MINILAB microcompounder (Thermo Electron Corporation, Germany) at 100 rpm over 5 min.

PBS/amino acid blends were obtained by the same protocol by changing only the weight ratio of organic molecule to 2% (w/w) ratio and by taking into account the relative content of molecule interleaved in LDH filler and dispersed in PBS nanocomposites.

Films were prepared by compression moulding between two Teflon sheets for one minute under 200 bar at 120 °C. The thickness of the films was about 50 to 60 μm.

XRD measurements were performed with a powder X-ray diffractometer (Philipps X-Pert Pro) and by using Cu-K_α radiation. Acquisition in the lower-angle domain started from 0.7 to 20° (2θ) with a step scan of 0.03 and a counting time of 10 s per step. Basal spacings were determined from the position of the harmonic reflections.

Nitrogen-adsorption isotherms determined at the temperature of liquid nitrogen (77 K) were performed with a Coulter SA3100 surface analyzer and the BET calculation method. The samples were previously outgassed under vacuum at 393 K for 300 min before each experiment.

UV/Vis spectra of the solids were obtained with a Shimadzu UV-2101 PC spectrophotometer equipped with an integrating sphere for diffuse reflection. The absorption was calculated from the diffuse reflectance spectra using Kubelka–Munk theory. The transmission mode was used with the same spectrophotometer to obtain transmittance spectra for PBS films blended with amino acid organically modified hydrotalcites.

Fluorescence spectra of PBS films were recorded with a Perkin–Elmer LS-55 luminescence spectrophotometer equipped with a front surface accessory and a pulsed xenon excitation source. Excitation was set at 280 nm and the emission signal was collected with the monochromator from 250 to 500 nm at a speed scan of 120 nm min^{-1}.

The melt rheological properties of the polymer blends were measured at 120 °C with a rotational spectrometer (ARES, TA, USA) equipped with a parallel plate geometry (plate diameter 8 mm, gap 1 mm). The imposed oscillatory shear stress amplitude was tested to validate the measurements inside the linear viscoelastic domain. This strain was fixed and used for measuring the dynamic stress against oscillatory shearing frequency (from 0.1 to 100 rad s^{-1}). G' (storage modulus), G'' (loss modulus) and $\tan\delta$ (ratio of G'' on G') were monitored automatically against frequency. The curve that represented the storage viscosity (η") against loss viscosity (η') is designated as the Cole–Cole plot. It was used to determine the Newtonian zero-shear viscosity η'_0 of PBS blends, which corresponds to the extrapolation from the convex downward and depressed semicircle for $\eta \rightarrow 0$. This value is proportional to the molecular weight M_r according to a α power-law relationship $\eta'_0 = K M_w^{\alpha}$.[36] The complex viscosity $|\eta^*|$ was also plotted against the shearing frequency ω. The shear-thinning parameter n was calculated in the low-ω region and by assuming that $|\eta^*|$ tends to ω^n.

Photoageing experiments on PBS nanocomposites were conducted with a device equipped with a mercury-vapour lamp (Novalamp RVC 400 W) that emits spectral rays above 295 nm. The emitting rays in the UV-B and UV-A region that correspond to an irradiance of 26 W m^{-2} was measured with an Ocean Optics SD 2000 CCD spectrophotometer.

Supporting Information (see footnote on the first page of this article): XRD spectrum of polybutylene succinate and irradiated polybutylene succinate nanocomposites, differential scanning calorimetry thermograms of irradiated polybutylene succinate nanocomposites, fluorescence spectra and rheological measurements of polybutylene succinate blends for various exposure times, shear thinning parameters in the low shearing frequency for polybutylene succinate blends and nanocomposites for various exposure times.

Acknowledgments

We thank the Ecole Nationale Supérieure de Chimie de Clermont-Ferrand (ENSCCF) for the financial support provided for this research.

[1] R. A. Gross, B. Kalra, *Science* **2002**, *297*, 803–807.
[2] M. Ishii, M. Okazaki, Y. Shibasaki, M. Ueda, T. Teranishi, *Biomacromolecules* **2001**, *2*, 1267–1270.
[3] S. Carrocio, P. Rizzarelli, C. Puglisi, G. Montaudo, *Macromolecules* **2004**, *37*, 6576–6586.
[4] N. T. Dintcheva, F. P. La Mantia, *Polym. Degrad. Stab.* **2007**, *92*, 630–634.
[5] E. Ruiz-Hitzky, P. Aranda, M. Darder, G. Rytwo, *J. Mater. Chem.* **2010**, *20*, 9306–9321.
[6] H. Yamada, K. Tamura, Y. Watanabe, N. Iyi, K. Morimoto, *Sci. Technol. Adv. Mater.* **2011**, *12*, 064705.
[7] G. Aloisi, U. Costantino, F. Elisei, L. Latterini, C. Natali, M. Nocchetti, *J. Mater. Chem.* **2002**, *12*, 3316–3323.

[8] S. He, T. Yin, T. Sato, *J. Phys. Chem. Solids* **2004**, *65*, 395–402.
[9] A. Illaik, C. Vuillermoz, S. Commereuc, C. Taviot-Guéhot, V. Verney, F. Leroux, *J. Phys. Chem. Solids* **2008**, *69*, 1362–1366.
[10] L. Tammaro, M. Tortora, V. Vittoria, U. Costantino, J. Marmottini, *J. Polym. Sci., Part A* **2005**, *43*, 2281–2290.
[11] Q. Zhou, V. Verney, S. Commereuc, I. J. Chin, F. Leroux, *J. Colloid Interface Sci.* **2010**, *349*, 127–133.
[12] S. S. Ray, P. Maiti, M. Okamoto, K. Yamada, K. Ueda, *Macromolecules* **2002**, *35*, 3104–3110.
[13] U. Costantino, M. Nocchetti, M. Sisani, R. Vivani, *Kristallographie* **2009**, *224*, 273–281.
[14] P. B. Messersmith, E. P. Giannelis, *J. Polym. Sci., Part A* **1995**, *33*, 1047–1057.
[15] P. Ding, B. Qu, *Polym. Eng. Sci.* **2006**, *46*, 1153–1159.
[16] R. Marangoni, L. Pereira Ramos, F. Wypych, *J. Colloid Interface Sci.* **2009**, *330*, 303–309.
[17] D. Li, Z. Tuo, D. G. Evans, X. Duan, *J. Solid State Chem.* **2006**, *179*, 3114–3120.
[18] U. Costantino, V. Bugatti, G. Gorrasi, F. Montanari, M. Nocchetti, L. Tammaro, V. Vittoria, *ACS Appl. Mater. Interfaces* **2009**, *1*, 668–677.
[19] U. Costantino, V. Ambrogi, M. Nocchetti, L. Perioli, *Microporous Mesoporous Mater.* **2008**, *107*, 149–160.
[20] C. Coelho, M. Hennous, V. Verney, F. Leroux, *RSC Adv.* **2012**, *2*, 5430–5438.
[21] M. Wei, S. Yuan, D. G. Evans, Z. Wang, X. Duan, *J. Mater. Chem.* **2005**, *15*, 1197–1203.
[22] T. Hibino, *Chem. Mater.* **2004**, *16*, 5482–5488.
[23] S. Aisawa, S. Takahashi, W. Ogasawara, Y. Umetsu, E. Narita, *J. Solid State Chem.* **2001**, *162*, 52–62.
[24] Y. Wang, P. Wu, B. Li, N. Zhou, Z. Zhang, *Appl. Clay Sci.* **2011**, *53*, 615.
[25] T. Kollar, I. Palinko, Z. Konya, I. Kiricsi, *J. Mol. Struct.* **2003**, *1*, 335–340.
[26] S. P. Newman, T. Di Cristina, P. V. Coveney, *Langmuir* **2002**, *18*, 2933–2939.
[27] M. X. Reinholdt, R. J. Kirkpatrick, *Chem. Mater.* **2006**, *18*, 2567–2576.
[28] J. F. Naime Filho, F. Leroux, V. Verney, J. Barros Valim, *Appl. Clay Sci.* **2012**, *55*, 88–93.
[29] A. Yasutake, S. Aisawa, S. Takahashi, H. Hirahara, E. Narita, *J. Phys. Chem. Solids* **2008**, *69*, 1542–1546.
[30] F. Belleza, A. Cipiciani, L. Latterini, T. Posati, P. Sassi, *Langmuir* **2009**, *25*, 10918–10924.
[31] R. Allmann, *Chimia* **1970**, *24*, 99.
[32] A. Fudala, I. Palinko, I. Kiricsi, *Inorg. Chem.* **1999**, *38*, 4653–4658.
[33] J. Bauer, P. Behrens, M. Speckbacher, H. Langhals, *Adv. Funct. Mater.* **2003**, *13*, 241–248.
[34] E. S. Yoo, S. S. Im, *J. Polym. Sci., Part B* **1999**, *37*, 1357–1366.
[35] L. Latterini, M. Nocchetti, G. G. Aloisi, U. Costantino, F. Elisei, *Inorg. Chim. Acta* **2007**, *360*, 728–740.
[36] H. H. Winter, *Gel Point in Encyclopedia of Polymer Science and Engineering*, New York, John Wiley & Sons, New York, **1989**.

Received: May 16, 2012
Published Online: September 12, 2012

